Microscopic Theory of Far-Infrared Two-Magnon Absorption in Antiferromagnets. I. Perturbation-Theory Search and Application of Fourth-Order Process to FeF_2

J. Woods Halley*
Department of Physics, University of California, Berkeley, California
(Received 1 October 1965; revised manuscript received 8 April 1966)

A microscopic description of the mechanism responsible for an absorption line observed in antiferromagnetic FeF_2 at 154 cm^{-1} is proposed. The mechanism appears to account for the properties of the observed line which are described in the preceding paper. In isolating the proposed mechanism, we set up a model which includes magnon, phonon, exciton, and photon fields and their interactions. The mechanism involves an indirect coupling between odd-parity excitons and magnons which we have previously called the odd-exciton-magnon interaction. This coupling is a consequence of the combined action of the spin-orbit interaction and the quadrupole-dipole part of the spin-orbit interaction. A search through fourth order in perturbation theory in this model yields several other possible processes. Our estimates indicate that the process we propose is the largest contributor in FeF_2 and that a third process, involving a phonon, may be contributing to the absorption intensity. The proposed process is used to derive the spin Hamiltonian used in the preceding paper and to estimate the intensity and polarization ratio.

I. INTRODUCTION

An absorption line has been found at the wave number 154.4 cm^{-1} in far-infrared-absorption studies of antiferromagnetic FeF_2.[1-4] In the preceding paper,[5] the properties of the line were described and a phenomenological theory explaining them was proposed. This theory postulated a spin Hamiltonian which we derive microscopically here. We develop a model which includes magnon, phonon, photon and exciton fields in zero order. The interactions include the usual magnon-phonon, spin-orbit, electric dipole, and crystal-field–phonon interactions, as well as the quadrupole-dipole part of the Coulomb interaction between the magnetic ions. The latter leads to an effective coupling between magnons and excitons of odd parity which we have previously[6] called the odd-exciton–magnon interaction and which is essential to the absorption mechanism proposed for the FeF_2 line. The physical source of this coupling and its order of magnitude can be understood from the following simple picture (though one must be careful[7] not to take this picture too literally). Consider an Fe^{2+} ion like that labeled j in Fig. 1 and two of its electronic energy levels, labeled o and e', which have odd and even parity, respectively, as well as two of its neighbors, labeled $j\pm\delta$ in the figure. If the ion at j is in a center of symmetry in the ground magnetic state of the system, the neighbors will not produce a coupling between the levels o and e'. Suppose that a magnon of large $\mathbf{k}$ is excited in the system in such a way that the spins of the neighboring ions $j\pm\delta$ precess as qualitatively indicated in the figure. A coupling between o and e' is then produced in the following way: The spins of the ions $j\pm\delta$ interact with their charge clouds via the spin-orbit interaction labeled L.S. The charge clouds of the ions on $j\pm\delta$ then interact in turn with the charge cloud of the ion at j via the quadrupole-dipole interaction labeled Q:T. Without considering, for the moment, the rather intricate question of whether this process gives a finite interaction when the time-reversal properties of the operators involved are fully considered, we can make a rough estimate of the order of magnitude of the coupling from this picture. The interaction will be of order

$$V\sim z(\lambda/\Delta)Q(a_Be/a^4),$$

where Q is a quadrupole moment $\sim ea_B^2$; a_B is the Bohr radius, z is the number of nearest neighbors, Δ is an energy of the order of the crystal-field splitting, λ is the spin-orbit coupling, and z is the number of neighbors. We have, with $\lambda\sim10^2$ cm^{-1}; $\Delta\sim10^3$ cm^{-1}; $z=8$, $a_B=0.5$ Å, $a=4$ Å,

$$V\sim20\ cm^{-1},$$

or about $\frac{1}{5}$ of the ordinary spin-orbit interaction.

The mechanism to which we attribute the line is indicated schematically in Fig. 2, where only the energy levels on a single ion j are shown. The external electromagnetic field couples the states e and o via the interaction $(-e/mc)\mathbf{A}\cdot\mathbf{p}$. The state o (or, more excatly, the corresponding exciton state) is coupled to a two-magnon state via the combined action of the even-odd coupling we have described and the spin-orbit interac-

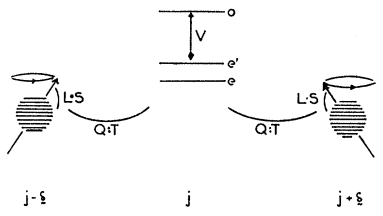

FIG. 1. Schematic illustration of the physical basis of the interaction.

* National Science Foundation Postdoctoral Fellow.
[1] I. Silvera, thesis, University of California, Berkeley, 1965 (unpublished).
[2] I. Silvera and M. Tinkham, Bull. Am. Phys. Soc. **1**, 714 (1964).
[3] P. L. Richards, Bull. Am. Phys. Soc. **10**, 33 (1965).
[4] R. C. Ohlman and M. Tinkham, Phys. Rev. **123**, 425 (1961).
[5] J. W. Halley and I. Silvera, preceding paper, Phys. Rev. **149**, 415 (1966).
[6] J. W. Halley and I. Silvera, Phys. Rev. Letters **15**, 654 (1965).
[7] Y. Tanabe, T. Moriya, and S. Sugano, Phys. Rev. Letters **15**, 1023 (1965).

tion on j. In the following we conduct a search in perturbation theory which indicates that this process is probably the largest contributor in FeF_2. Using it, the the spin Hamiltonian of the previous paper is derived and the intensity of the FeF_2 line is estimated. Finally, we discuss the results, their relationship to other theories and experiments, and the realm of applicability of the ideas presented here.

II. ZERO-ORDER HAMILTONIAN

The FeF_2 system consists of Fe^{2+} ions and F^- ions in a rutile structure; the orbital ground state of the Fe^{2+} ion is $(3d)^6\ {}^5D$. This state is split in the crystal field[8,9] as shown in Fig. 3, after Ref. 8. The energies are known only very approximately. The symmetry properties characterizing the wave functions in Fig. 3 are expressed in terms of the coordinate system x, y, z of Fig. 1 of the preceding paper. The Fe^{2+} spins order antiferromagnetically below 78°K as shown there. We write the zero-order Hamiltonian describing this system in the form

$$\mathcal{H}_0=\mathcal{H}_{\text{magnons}}+\mathcal{H}_{\text{phonons}}+\mathcal{H}_{\text{excitons}}+\mathcal{H}_{\text{photons}}. \quad (1)$$

Here

$$\mathcal{H}_{\text{magnons}}=\sum_{\mathbf{k}} \hbar\omega_{\mathbf{k}}{}^{m}(\alpha_{\mathbf{k}}{}^{\dagger}\alpha_{\mathbf{k}}+\beta_{\mathbf{k}}{}^{\dagger}\beta_{\mathbf{k}}) \quad (2)$$

is derived from the FeF_2 spin Hamiltonian (1) of the preceding paper via the transformations (3) of the preceding paper and a Bogoliubov transformation which is an identity near the Brillouin-zone boundary. $\omega_{\mathbf{k}}{}^{m}$ is the magnon frequency and $\alpha_{\mathbf{k}}$, $\alpha_{\mathbf{k}}{}^{\dagger}$ and $\beta_{\mathbf{k}}$, $\beta_{\mathbf{k}}{}^{\dagger}$ are magnon destruction and creation operators with boson commutation relations. The expression is valid in zero magnetic field at low temperatures. The sum is over all wave vectors on the reciprocal sublattice.

For the phonon part of the zero-order Hamiltonian, we have

$$\mathcal{H}_{\text{phonons}}=\sum_{\mathbf{q},p} \hbar\omega_{\mathbf{q},p}A_{\mathbf{q},p}{}^{\dagger}A_{\mathbf{q},p}. \quad (3)$$

The A's are phonon annihilation and creation operators related to the normal mode momenta and coordinates of the ions via relations given in Ref. 10. The sum over wave vectors is over the reciprocal lattice. p is a polarization index taking values 1, 2, 3. In the present work we will only treat phonons via rough order-of-magnitude estimates and hence will not need the detailed relations between the A's and the ionic coordinates.

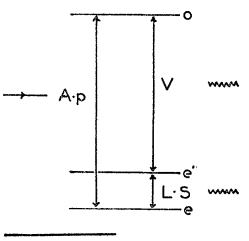

FIG. 2. Schematic illustration of the process to which the observed absorption is attributed.

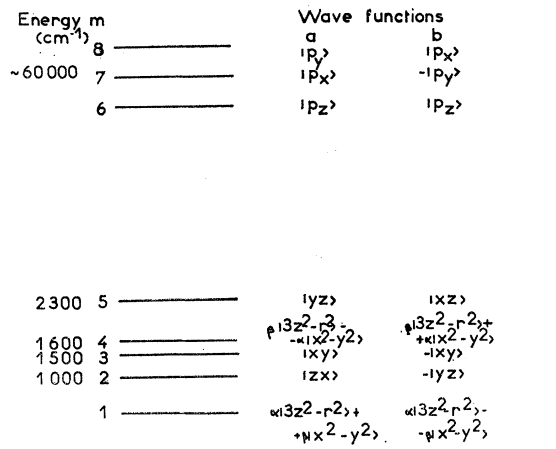

FIG. 3. Energy levels of the Fe^{2+} ion. The wave functions are referred to the coordinate system x, y, z of Fig. 1 of the preceding paper.

For the exciton Hamiltonian we have, from Appendix A,

$$\mathcal{H}_{\text{excitons}}=\sum_{m,\mathbf{k}}{}' E_m(\beta_{\mathbf{k}}{}^{(m,a)\dagger}\beta_{\mathbf{k}}{}^{(m,a)}+\beta_{\mathbf{k}}{}^{(m,b)\dagger}\beta_{\mathbf{k}}{}^{(m,b)}). \quad (4)$$

Here m is an index labeling the single-ion state of which the corresponding exciton is a phased linear combination. The β's are defined in Appendix A, The prime on the sum means that $m=1$ (corresponding to the single-ion ground state) is to be excluded. The energies E_m are the single-ion energies in the approximation (which we will use) in which exciton dispersion is neglected. The sum over $\mathbf{k}$ is over the reciprocal sublattice. The β's satisfy boson commutation relations to a good approximation.[11]

The electromagnetic field is described by

$$\mathcal{H}_{\text{photons}}=\sum_{\mathbf{k},\lambda} hc|\mathbf{k}|a_{\mathbf{k}\lambda}{}^{\dagger}a_{\mathbf{k}\lambda}, \quad (5)$$

where the vector potential is

$$\mathbf{A}(\mathbf{x})=\frac{1}{V^{1/2}}\sum_{\mathbf{k},\lambda}\left(\frac{2\pi\hbar c}{k}\right)^{1/2}\hat{\epsilon}_{\mathbf{k}\lambda}(a_{\mathbf{k}\lambda}e^{-i\mathbf{k}\cdot\mathbf{x}}+a_{\mathbf{k}\lambda}{}^{\dagger}e^{i\mathbf{k}\cdot\mathbf{x}}) \quad (6)$$

at the point $\mathbf{x}$. Here V is the crystal volume; $\hat{\epsilon}_{\mathbf{k}\lambda}$ is the photon polarization vector and λ is a polarization index taking values 1, 2. The sum over $\mathbf{k}$ is over the set $2\pi\hat{n}/V^{1/3}$; $\hat{n}=(n_x,n_y,n_z)$; $n_i=0, 1, 2,\cdots$.

[8] T. Moriya *et al.*, J. Phys. Soc. Japan **11**, 211 (1956).
[9] C. Moore, Natl. Bur. Std. U. S. Circ. 467, Vol. II, 61 (1952).
[10] J. M. Ziman, *Electrons and Phonons* (Clarendon Press, Oxford, England, 1962), p. 50.
[11] This can be shown by arguments like those in P. W. Anderson, *Concepts in Solids* (W. A. Benjamin, Inc., New York, 1963), p. 132.

III. INTERACTIONS

In this section we label the ionic wave functions of states of energy E_m of ions on the two sublattices of the antiferromagnetic by $|\Gamma_j{}^m\rangle_a$ and $|\Gamma_{j+\tau}{}^m\rangle_b$ or by $|m\rangle_a$ and $|m\rangle_b$.

The interaction between photons and excitons arises from the $\mathbf{A}\cdot\mathbf{p}$ term in the low-energy form of the Dirac equation

$$\frac{-e}{mc}\sum_{j=1}^{2N}\sum_{l=1}^{6}\mathbf{P}_j{}^{(l)}\cdot\mathbf{A}(\mathbf{x}_j{}^{(l)},t),$$

by an expansion of $\mathbf{A}$ about the points $\mathbf{x}_j{}^{(l)}=\mathbf{R}_j{}^{(0)}$, where $\mathbf{R}_j{}^{(0)}$ is the position of the jth ion. From this, we derive the exciton-photon interaction

$$\begin{aligned}\mathcal{H}_{\text{ex-phot}}=&\frac{-ie}{(2N\Omega)^{1/2}}\sum_{\substack{\mathbf{k},\mathbf{k}',\lambda\\ m,m'}}\left(\frac{2\pi\hbar}{ck}\right)^{1/2}\{(\mathbf{X}^{(a)}(m,m')\cdot\hat{\epsilon}_{\mathbf{k}\lambda})\omega(m',m)(\beta_{\mathbf{k}'}{}^{(m,a)\dagger}\beta_{\mathbf{k}'-\mathbf{k}}{}^{(m',a)}a_{\mathbf{k}\lambda}+\beta_{\mathbf{k}'}{}^{(m,a)\dagger}\beta_{\mathbf{k}+\mathbf{k}'}{}^{(m',a)}a_{\mathbf{k}\lambda})\\&+(\mathbf{X}^{(b)}(m,m')\cdot\hat{\epsilon}_{\mathbf{k}\lambda})\omega(m',m)(\beta_{\mathbf{k}'}{}^{(m,b)\dagger}\beta_{\mathbf{k}'-\mathbf{k}}{}^{(m',b)}a_{\mathbf{k}\lambda}+\beta_{\mathbf{k}'}{}^{(m,b)\dagger}\beta_{\mathbf{k}+\mathbf{k}'}{}^{(m',b)}a_{\mathbf{k}\lambda}{}^{\dagger})\}+\frac{(-ie)}{(2\Omega)^{1/2}}\sum_{\mathbf{k},\lambda}\sum_{m}\left(\frac{2\pi\hbar}{ck}\right)^{1/2}\\&\times\{(\mathbf{X}^{(a)}(m,1)\cdot\hat{\epsilon}_{\mathbf{k}\lambda})\omega(1,m)(\beta_{\mathbf{k}}{}^{(m,a)\dagger}a_{\mathbf{k}\lambda}+\beta_{-\mathbf{k}}{}^{(m,a)\dagger}a_{\mathbf{k}\lambda}{}^{\dagger})+(\mathbf{X}^{(a)}(1,m)\cdot\hat{\epsilon}_{\mathbf{k}\lambda})\omega(m,1)(\beta_{-\mathbf{k}}{}^{(m,a)}a_{\mathbf{k}\lambda}+\beta_{\mathbf{k}}{}^{(m,a)}a_{\mathbf{k}\lambda}{}^{\dagger})\\&+(\mathbf{X}^{(b)}(m,1)\cdot\hat{\epsilon}_{\mathbf{k}\lambda})\omega(1,m)(\beta_{\mathbf{k}}{}^{(m,b)\dagger}a_{\mathbf{k}\lambda}+\beta_{-\mathbf{k}}{}^{(m,b)\dagger}a_{\mathbf{k}\lambda}{}^{\dagger})+(\mathbf{X}^{(b)}(1,m)\cdot\hat{\epsilon}_{\mathbf{k}\lambda})\omega(1,m)(\beta_{-\mathbf{k}}{}^{(m,b)}a_{\mathbf{k}\lambda}+\beta_{\mathbf{k}}{}^{(m,b)}a_{\mathbf{k}\lambda}{}^{\dagger})\}.\end{aligned}\tag{7}$$

In this expression

$$\mathbf{X}^{(a)}(m,m')=\langle\Gamma_j{}^m|_a\sum_{l=1}^{6}(\mathbf{x}_j{}^{(l)}-\mathbf{R}_j{}^{(0)})|\Gamma_j{}^{m'}\rangle_a;$$

$$\mathbf{X}^{(b)}(m,m')=\langle\Gamma_{j+\tau}{}^m|_b\sum_{l=1}^{6}(\mathbf{x}_{j+\tau}{}^{(l)}-\mathbf{R}_{j+\tau}{}^{(0)})|\Gamma_{j+\tau}{}^{m'}\rangle_b;$$

$$\omega(m',m)=(1/\hbar)[E(m')-E(m)].$$

Ω is the volume of the unit cell.

The mechanism leading to a direct magnon-exciton interaction is the spin-orbit interaction, which we write in the form[12]

$$\mathcal{H}_{\text{spin-orbit}}=\lambda\sum_{j=1}^{2N}\mathbf{L}_j\cdot\mathbf{S}_j,$$

where $\mathbf{L}_j=\sum_{l=1}^{6}\mathbf{l}_j{}^{(l)}$ for the jth ion and $\mathbf{l}_j{}^{(l)}$ is the angular momentum operator of the lth electron of the jth ion. The sum is over all the ions of the crystal. The resultant magnon-exciton interaction includes the following terms, which are of interest in the present problem:

$$\begin{aligned}\mathcal{H}_{\text{ex-mag}}=\lambda(S/2)^{1/2}\sum_{\mathbf{k}}\{&(\langle 1|_aL^+|m\rangle_ac_{\mathbf{k}}{}^{\dagger}+\langle 1|_aL^-|m\rangle_ac_{-\mathbf{k}})\beta_{\mathbf{k}}{}^{(m,a)}+(\langle m|_aL^+|1\rangle_ac_{-\mathbf{k}}{}^{\dagger}+\langle m|_aL^-|1\rangle_ac_{\mathbf{k}})\beta_{\mathbf{k}}{}^{(m,a)\dagger}\\&+(\langle 1|_bL^+|m\rangle_bd_{-\mathbf{k}}+\langle 1|_bL^-|m\rangle_bd_{\mathbf{k}}{}^{\dagger})\beta_{\mathbf{k}}{}^{(m,b)}+(\langle m|_bL^+|1\rangle_bd_{\mathbf{k}}+\langle m|_bL^-|1\rangle_bd_{-\mathbf{k}}{}^{\dagger})\beta_{\mathbf{k}}{}^{(m,b)\dagger}\}.\end{aligned}\tag{8}$$

(The other terms arising from $\mathcal{H}_{\text{spin-orbit}}$ were considered in the search described in the next section.) Here $c_{\mathbf{k}}$ and $d_{\mathbf{k}}$ are defined in terms of the spin operators by Eqs. (3) of the preceding paper.

The effective coupling between excitons of odd parity and magnons arises as a consequence of the combined action of the spin-orbit interaction and the quadrupole-dipole interaction between the magnetic ions. The latter has the form

$$\mathcal{H}_{\text{quad-dip}}=e^2\sum_{j,\delta}(\mathbf{Q}_j:\mathbf{T}_{\delta,j+\delta}+\mathbf{Q}_{j+\tau}:\mathbf{T}_{\delta,j+\tau}),\tag{9}$$

where

$$\begin{aligned}\mathbf{Q}_j=&\sum_{\mu=1}^{6}[3(\mathbf{x}_j{}^{(\mu)}-\mathbf{R}_j{}^{(0)})(\mathbf{x}_j{}^{(\mu)}-\mathbf{R}_j{}^{(0)})-\mathbf{1}(\mathbf{x}_j{}^{(\mu)}-\mathbf{R}_j{}^{(0)})^2];\\\mathbf{T}_{j,\delta}=&\tfrac{1}{2}\sum_{\mu=1}^{6}\left[\frac{5\boldsymbol{\delta}\boldsymbol{\delta}}{|\boldsymbol{\delta}|^7}(\mathbf{x}_{j+\delta}{}^{(\mu)}-\mathbf{R}_j{}^{(0)})\cdot\boldsymbol{\delta}-\left(\frac{\boldsymbol{\delta}(\mathbf{x}_{j+\delta}{}^{(\mu)}-\mathbf{R}_j{}^{(0)})+(\mathbf{x}_{j+\delta}{}^{(\mu)}-\mathbf{R}_j{}^{(0)})\boldsymbol{\delta}}{|\boldsymbol{\delta}|^5}\right)\right].\end{aligned}\tag{10}$$

[12] This form is valid for states of the Fe^{2+} ion with $S=2$ for the spin state. This excludes some high-lying even states of the $(3d)^6$ configuration which will, however, not appear in the process we consider.

From this one finds an exciton-exciton interaction

$$\mathcal{H}_{\text{ex-ex}}=\frac{2ie^2}{N}\sum_{\substack{m,m'\\m''m'''}}{}'\sum_{\delta}{}'\sum_{\mathbf{k},\mathbf{k}',\mathbf{k}''}[(\langle m|{}_a\mathbf{Q}|m'\rangle_a:\langle m''|{}_b\mathbf{T}_\delta|m'''\rangle_b$$

$$-\langle m''|{}_b\mathbf{Q}|m'''\rangle_b)\sin[(\mathbf{k}-\mathbf{k}')\cdot\boldsymbol{\delta}]\beta_{\mathbf{k}}{}^{(m,a)\dagger}\beta_{\mathbf{k}'}{}^{(m',a)}\beta_{\mathbf{k}''}{}^{(m'',b)\dagger}\beta_{\mathbf{k}''-\mathbf{k}'+\mathbf{k}}{}^{(m''',b)}]$$

$$+\frac{2ie^2}{N^{1/2}}\sum_{\substack{m,m''\\m'''}}{}'\sum_{\delta}{}'\sum_{\mathbf{k},\mathbf{k}'}[\beta_{\mathbf{k}'}{}^{(m'',b)\dagger}(-\langle m|{}_a\mathbf{Q}|1\rangle_a:\langle m''|{}_b\mathbf{T}_\delta|m'''\rangle_b$$

$$\times\beta_{\mathbf{k}}{}^{(m,a)\dagger}\beta_{\mathbf{k}+\mathbf{k}'}{}^{(m''',b)}+\langle 1|{}_a\mathbf{Q}|m\rangle_a:\langle m''|{}_bT_\delta|m'''\rangle_b\beta_{\mathbf{k}}{}^{(m,a)}\beta_{\mathbf{k}'-\mathbf{k}}{}^{(m''',b)})$$

$$\times\sin(\mathbf{k}\cdot\boldsymbol{\delta})+\beta_{\mathbf{k}'}{}^{(m'',a)\dagger}(-\langle m|{}_b\mathbf{Q}|1\rangle_b:\langle m''|{}_aT_\delta|m'''\rangle_a\beta_{\mathbf{k}}{}^{(m,b)\dagger}\beta_{\mathbf{k}+\mathbf{k}'}{}^{(m''',a)}$$

$$+\langle 1|{}_b\mathbf{Q}|m\rangle_b:\langle m''|{}_a\mathbf{T}_\delta|m'''\rangle_a\beta_{\mathbf{k}}{}^{(m,b)}\beta_{-\mathbf{k}+\mathbf{k}'}{}^{(m''',a)})\sin(\mathbf{k}\cdot\boldsymbol{\delta})$$

$$+\beta_{\mathbf{k}'}{}^{(m'',a)}(-\langle m|{}_a\mathbf{Q}|m''\rangle_a:\langle m'''|{}_b\mathbf{T}_\delta|1\rangle_b\beta_{\mathbf{k}}{}^{(m,a)\dagger}\beta_{-\mathbf{k}+\mathbf{k}'}{}^{(m''',b)\dagger}$$

$$+\langle m|{}_a\mathbf{Q}|m''\rangle_a:\langle 1|{}_b\mathbf{T}_\delta|m''\rangle_b\beta_{\mathbf{k}}{}^{(m,a)\dagger}\beta_{\mathbf{k}-\mathbf{k}'}{}^{(m''',b)})\sin[(\mathbf{k}-\mathbf{k}')\cdot\boldsymbol{\delta}]$$

$$+\beta_{\mathbf{k}}{}^{(m,b)\dagger}(-\langle m|{}_b\mathbf{Q}|m''\rangle_b:\langle m'''|{}_a\mathbf{T}_\delta|1\rangle_a\beta_{\mathbf{k}'}{}^{(m'',b)}\beta_{\mathbf{k}'-\mathbf{k}}{}^{(m''',a)\dagger}$$

$$+\langle m|{}_b\mathbf{Q}|m'''\rangle_b:\langle 1|{}_a\mathbf{T}_\delta|m'''\rangle_a\beta_{\mathbf{k}'}{}^{(m'',b)}\beta_{\mathbf{k}-\mathbf{k}'}{}^{(m''',a)})\sin[(\mathbf{k}-\mathbf{k}')\cdot\boldsymbol{\delta}]]$$

$$+2ie^2\sum_{m,m'}{}'\sum_{\delta}{}'\sum_{\mathbf{k}}[(-\langle m|{}_a\mathbf{Q}|1\rangle_a:\langle m''|{}_b\mathbf{T}_\delta|1\rangle_b$$

$$+\langle m''|{}_b\mathbf{Q}|1\rangle_b:\langle m|{}_a\mathbf{T}_\delta|1\rangle_a)\sin(\mathbf{k}\cdot\boldsymbol{\delta})\beta_{\mathbf{k}}{}^{(m,a)\dagger}\beta_{-\mathbf{k}}{}^{(m'',b)\dagger}$$

$$+(-\langle m|{}_a\mathbf{Q}|1\rangle_a:\langle 1|{}_b\mathbf{T}_\delta|m''\rangle_b+\langle 1|{}_b\mathbf{Q}|m''\rangle_b:\langle m|{}_a\mathbf{T}_\delta|1\rangle_a)\sin(\mathbf{k}\cdot\boldsymbol{\delta})\beta_{\mathbf{k}}{}^{(m,a)\dagger}\beta_{\mathbf{k}}{}^{(m'',b)}$$

$$+(\langle 1|{}_a\mathbf{Q}|m\rangle_a:\langle m''|{}_b\mathbf{T}_\delta|1\rangle_b-\langle m''|{}_b\mathbf{Q}|1\rangle_b:\langle 1|{}_a\mathbf{T}_\delta|m\rangle_a)\sin(\mathbf{k}\cdot\boldsymbol{\delta})\beta_{\mathbf{k}}{}^{(m,a)}\beta_{\mathbf{k}}{}^{(m'',b)\dagger}$$

$$+(\langle 1|{}_a\mathbf{Q}|m\rangle_a:\langle 1|{}_b\mathbf{T}_\delta|m''\rangle_b-\langle 1|{}_b\mathbf{Q}|m''\rangle_b:\langle 1|{}_a\mathbf{T}_\delta|m\rangle_a)\sin(\mathbf{k}\cdot\boldsymbol{\delta})\beta_{\mathbf{k}}{}^{(m,a)}\beta_{-\mathbf{k}}{}^{(m'',b)})]. \quad (11)$$

In the next section we will include the following interactions, in addition to those given above: the electric dipole interaction between photons and optical phonons; the exciton-phonon interaction arising from the nuclear coordinate dependence of the crystal field; the "exchange-striction" part[13] of the magnon-phonon interaction; the lowest order relativistic correction to (7); the magnetic dipole interaction between magnons and photons and the dependence of the exchange integral J on the E field of the radiation field. These interactions are estimated in order of magnitude in the next section, where we conclude that their explicit forms are not needed for the FeF_2 problem. The system which we consider, including the interactions just mentioned, is schematically sketched in Fig. 4.

A formalism for doing perturbation theory on this system is set up in Appendix B. Definitions of the diagrams to be used in the next section are given there.

[13] The "Van Vleck" magnon-phonon interaction, arising from the combined interaction of the spin-orbit interaction and the dependence of the crystal field on the positions of the nuclei, is included in this model by consideration of both the latter interactions.

IV. POSSIBLE TWO-MAGNON AND MAGNON-PHONON ABSORPTION PROCESSES

We find possible processes by a systematic search. Of the five first-order absorption processes in the model, only that shown[14] diagrammatically[15] in Fig. 5 will give absorption near the observed frequency. The interaction is from the electric field dependence of the exchange interaction J. In Appendix C, the ratio of the absorption intensity from this process to that from the antiferromagnetic resonance absorption[16] (AFMR) is esti-

[14] This process is similar to that recently proposed independently by Tanabe *et al.* (Ref. 7) to explain the same experiments. The author is indebted to Professor C. Kittel for pointing out this process to him.

[15] Diagrams with the vertices in inverted order, though considered in Appendix D, are not considered in the estimates described in this section. They can appreciably increase the intensity in third and fourth orders and, in other cases can introduce cancellations which cause the net absorption to vanish. These considerations do not change the essential conclusions of the discussion.

[16] The ratio of the matrix elements is estimated. Because the magnetic-dipole interaction produces magnons nondispersively, the ratio observed experimentally will be larger. See, e.g., E. H. Jacobsen and K. W. H. Stevens, Phys. Rev. 129, 2036 (1962).

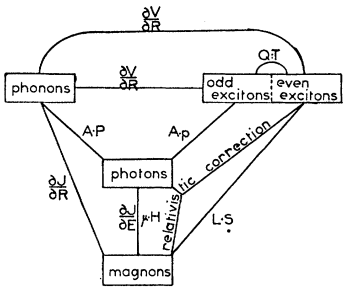

FIG. 4. Illustration of elements included in the model.

mated, using the Anderson[17] theory for the superexchange constant J. The result is

$$(\text{Intensity from } \partial J/\partial E)/\text{AFMR}\sim 5\times 10^{-10}\,.$$

In this estimate some terms involving off-diagonal exchange-type integrals which may be important have not been included. Thus the estimate cannot be regraded as conclusive in eliminating this process as a possible contributor to the absorption. Because it was so small, however, we extended the search to higher orders in perturbation theory.

FIG. 5. First-order process.

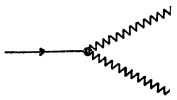

In second order, we find eleven electric dipole absorption processes of which only the one shown in Fig. 6 would give absorption near the observed absorption frequency. The interaction at the second vertex is the exchange-strictive part of the magnon-phonon part of the magnon-phonon interaction. To estimate it, we set

$$\mathcal{H}_{\text{mag-ph}}\sim(\partial J/\partial R)zS\delta R\,,$$

where z is the number of nearest neighbors, S is the spin, J is the exchange coupling, R is the position of the ion, and δR is the mean displacement when an optical phonon is excited. To estimate δR, we use $\omega_p\sim 10^{13}$ sec^{-1} for the phonon frequency and find $\delta R/a\sim 10^{-3}$, where a is the lattice constant. Writing $(\partial J/\partial R)\delta R\sim(\delta R/a)J$ and using $SzJ\sim 20$ cm^{-1} gives $\mathcal{H}_{\text{mag-ph}}\sim 2\times 10^{-2}$ cm^{-1}. The excited-excited intermediate state of the process lies $\sim 10^2$ cm^{-1} above ground. Thus

$$(\text{Intensity of process in Fig. 6})/\text{AFMR}\sim 10^{-4}, \quad (12)$$

including a factor of $\alpha_{\text{f.s.}}{}^{-2}\sim 10^4$ to account for the ratio of magnetic to electric dipole transition intensities. It is to be noted that if, as reported in some estimates,[18] the

FIG. 6. Second-order process.

[17] P. W. Anderson, Phys. Rev. **79**, 350 (1950).
[18] Y. Tanabe and S. Sugano, J. Phys. Soc. Japan **9**, 753 (1954).

FIG. 7. Third-order processes.

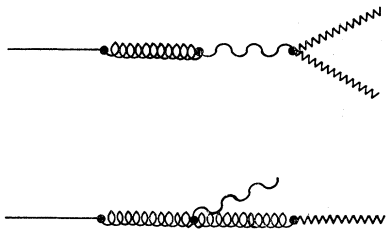

ratio $\delta R/a$ is closer to 10^{-1} than to 10^{-3}, then the ratio (12) would become one and the process might give sufficient absorption intensity to explain the experiments.

In third order, we find 44 electric dipole absorption processes of which the two shown in Fig. 7 correspond to absorption of a photon in the observed frequency range. The first of these has intensity of order $(V_{\text{cry}}(\delta R/a)/E_0)^2$ smaller that that of the process of Fig. 6. Here V_{cry} is of the order of the crystal-field energy or $\sim 10^3$ cm^{-1} and E_0 is the energy of the excited odd state $\sim 5\times 10^4$ cm^{-1}. With $\delta R/a\sim 10^{-3}$ this gives an intensity of 10^{-9} times that of the process of Fig. 6. For the second process of Fig. 7, we estimate the absorption frequency to be ~ 280 cm^{-1} if the phonon is acoustic, and ~ 350 cm^{-1} if the phonon is optical. The intensity of this second process is of order

$$10^4\left(\frac{V_{\text{cry}}(\delta R/a)}{E_0}\right)^2\left(\frac{\lambda}{E_e}\right)^2\sim 10^{-6}$$

times smaller than the AFMR absorption intensity. Here we take $\lambda\sim 10^2$ cm^{-1} and E_e, the energy of a low-lying even-parity orbital state $\sim 10^3$ cm^{-1}. Thus we conclude that neither third-order process will explain the experiments.

Of the 474 electric dipole absorption processes which we find in fourth order in this model, 22 might give absorption in the observed frequency range. Of these, 11 involve the electric-field dependence of J which we have already estimated to give a small first-order contribution to the absorption. The expressions for the absorption intensity arising from five others contain factors appearing in the corresponding second-order

FIG. 8. Fourth-order processes.

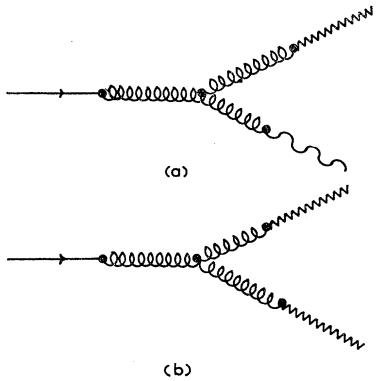

process of Fig. 6 in addition to new factors which are $\ll 1$. The matrix elements for three of the remaining processes involve a factor $\sim \sin k_{\rm ph} a$, where $k_{\rm ph}$ is the photon wave number and a is of the order of the lattice constant. In the FeF_2 problem, $\sin k_{\rm ph} a \sim 10^{-5}$. As a consequence, these are found to give absorption intensities of order 10^{-10} smaller than the two remaining fourth-order processes, which are shown diagrammatically in Fig. 8. To compare these we note that the ratio of intensities is of order $I_b/I_a \sim (\lambda/V_{\rm cry}(\delta R/a))^2 \sim 10^4$. Thus we consider the second process in Fig. 8. In order of magnitude we estimate that

$$I_b/\mathrm{AFMR} \sim \left(\frac{zQT\lambda^2 n}{E_0 E_e^2}\right)^2 \alpha_{\rm f.s.}^{-2}.$$

Here z is the number of neighbors and n is the number of terms appearing in the fourth-order perturbation calculation. The latter is $\sim 4! = 24$ and is thus significant. For QT we take $e^2/a_B(a_B/a)^4 \sim 16$ cm^{-1}. Thus

$$I_b/\mathrm{AFMR} \sim 2\times 10^{-3}.$$

This is larger than the intensities estimated for the other processes considered.

The search through order in perturbation theory thus yields two possible processes, one in fourth order and the other in second order, of which the first is estimated to give the largest contribution in the case of FeF_2. The processes appear diagrammatically in Figs. 6 and 8(b). We next consider the properties of the line which are predicted by the process of Fig. 8(b).

V. PROPERTIES PREDICTED BY THE FOURTH-ORDER PROCESS

We derive a detailed expression for the intensity given by the process for the general case of a two-sublattice antiferromagnet. The required calculations are described in Appendix D with the result

$$\begin{aligned}
&W(1_{\mathbf{k},\lambda}{}^{\rm photon} \longrightarrow 1_{\mathbf{k}'+\mathbf{k}}{}^{\rm magnon,a},\ 1_{-\mathbf{k}'}{}^{\rm magnon,b}) \\
&= (2\pi/\hbar^2)\delta(\omega_{\mathbf{k}\lambda}{}^{\rm ph} - \omega_{\mathbf{k}+\mathbf{k}'}{}^{\rm mag} - \omega_{-\mathbf{k}'}{}^{\rm mag}) \Bigg| \sum_{m_{e'},m_0,m_{e''}}{}' \Bigg\{ \frac{\lambda^2 e^3 S\omega(m_0,1)}{(V)^{1/2}} \hbar\omega_{\mathbf{k}\lambda}{}^{\rm ph} \left(\frac{2\pi\hbar}{\omega_{\mathbf{k}\lambda}{}^{\rm ph}}\right)^{1/2} \\
&\times \Big(\sum_\delta{}' \sin(\mathbf{k}'\cdot\boldsymbol{\delta}) \langle 1|{}_b\mathbf{Q}|m_{e'}\rangle_b : \langle m_0|{}_a\mathbf{T}_\delta|m_{e''}\rangle_a \langle m_{e'}|{}_bL^-|1\rangle_b \langle m_{e''}|{}_aL^+|1\rangle_a (\mathbf{X}^{(a)}(1,m_0)\cdot\hat{\epsilon}_{\mathbf{k}\lambda}) \\
&- \sum_\delta{}' \sin(\mathbf{k}'\cdot\boldsymbol{\delta}) \langle 1|{}_a\mathbf{Q}|m_{e'}\rangle_a : \langle m_0|{}_b\mathbf{T}_\delta|m_{e''}\rangle_b \langle m_{e'}|L^+|1\rangle_a \langle m_{e''}|{}_bL^-|1\rangle_b (\mathbf{X}^{(b)}(1,m_0)\cdot\hat{\epsilon}_{\mathbf{k}\lambda})\Big) \\
&\times M^{(1)}(m_{e'},m_{e''},m_0) + \frac{\lambda^2 S e^3 \omega(m_{e''},m_0)}{(V)^{1/2}} \hbar\omega_{\mathbf{k}\lambda}{}^{\rm ph} \left(\frac{2\pi\hbar}{\omega_{\mathbf{k}\lambda}{}^{\rm ph}}\right)^{1/2} \Big(\sum_\delta{}' \sin(\mathbf{k}'\cdot\boldsymbol{\delta}) \langle 1|{}_b\mathbf{Q}|m_{e'}\rangle_b : \langle 1|{}_a\mathbf{T}_\delta|m_0\rangle_a \\
&\times \langle m_{e''}|{}_aL^+|1\rangle_a \langle m_{e'}|L^-|1\rangle_b (\mathbf{X}^{(a)}(m_0,m_{e''})\cdot\hat{\epsilon}_{\mathbf{k}\lambda}) - \sum_\delta{}' \sin(\mathbf{k}\cdot\boldsymbol{\delta}) \langle 1|{}_a\mathbf{Q}|m_{e'}\rangle_a : \langle 1|{}_b\mathbf{T}_\delta|m_0\rangle_b \\
&\times \langle m_{e'}|{}_aL^+|1\rangle_a \langle m_{e''}|{}_bL^-|1\rangle_b (\mathbf{X}^{(b)}(m_0,m_{e''})\cdot\hat{\epsilon}_{\mathbf{k}\lambda}) M^{(2)}(m_{e'},m_{e''},m_0)\Bigg\}\Bigg|^2. \qquad (13)
\end{aligned}$$

Here $M^{(1)}(m_{e'},m_{e''},m_0)$ and $M^{(2)}(m_{e'},m_{e''},m_0)$ are defined in Appendix E and W is the transition rate. The calculation required to find the detailed form of this in the case of FeF_2 is described in Appendix E and we find

$$\begin{aligned}
&W(1_{\mathbf{k}\lambda}{}^{\rm photon} \longrightarrow 1_{\mathbf{k}'+\mathbf{k}}{}^{\rm magnon,a},\ 1_{-\mathbf{k}'}{}^{\rm magnon,x}) = \frac{2\pi}{\hbar^2}\delta(\omega_{\mathbf{k}\lambda}{}^{\rm ph} - 2\omega_{\mathbf{k}'}{}^{\rm mag}) \Bigg| \left(\frac{2\pi\hbar\omega_{\mathbf{k}\lambda}}{V}\right)^{1/2} (4S) \\
&\times \sum_\delta{}' \{\epsilon_{\mathbf{k}\lambda}{}^{(z)} P_0 \delta_z(\delta_x{}^2 - \delta_y{}^2) + \epsilon_{\mathbf{k}\lambda}{}^{(x)}(iP_2\delta_y + P_1\delta_x)|\boldsymbol{\delta}|^2 - \epsilon_{\mathbf{k}\lambda}{}^{(y)}(P_1\delta_y + iP_2\delta_x)|\boldsymbol{\delta}|^2\} \sin(\mathbf{k}'\cdot\boldsymbol{\delta})\Bigg|^2, \qquad (14)
\end{aligned}$$

where P_0, P_1, P_2 are given by Eqs. (E1) and (E2) of Appendix E. An effective "spin Hamiltonian" which gives the same result as (14) is given by

$$\begin{aligned}
\mathcal{H}_{\rm spin} = \sum_{\mathbf{k}'} \sum_\delta{}' \Bigg[&\left(\frac{2\pi\hbar\omega_{\mathbf{k}\lambda}}{V}\right)^{1/2} (4S)(a_{\mathbf{k}\lambda}{}^\dagger - a_{\mathbf{k}\lambda}) \sin(\mathbf{k}'\cdot\boldsymbol{\delta}) (\{\epsilon_{\mathbf{k}\lambda}{}^{(z)} P_0 \delta_z(\delta_x{}^2 - \delta_y{}^2) + (\epsilon_{\mathbf{k}\lambda}{}^{(x)}\delta_x - \epsilon_{\mathbf{k}\lambda}{}^{(y)}\delta_y) P_1 |\boldsymbol{\delta}|^2\} \\
&\times \{c_{\mathbf{k}'}{}^\dagger d_{-\mathbf{k}'}{}^\dagger - c_{\mathbf{k}'} d_{-\mathbf{k}'}\} + i\{\epsilon_{\mathbf{k}\lambda}{}^{(x)}\delta_y - \epsilon_{\mathbf{k}\lambda}{}^{(y)}\delta_x\} P_2 |\boldsymbol{\delta}|^2 \{c_{\mathbf{k}'}{}^\dagger d_{-\mathbf{k}'}{}^\dagger + c_{\mathbf{k}'} d_{-\mathbf{k}'}\}\Bigg]. \qquad (15)
\end{aligned}$$

Inverting this by use of the inverse of the transformations (3) of the preceding paper gives Eq. (2) of the preceding

paper, from which the properties of the experimental line are derived. In the evaluation of the polarization ratio in that work, the constants P_0/P_1 and P_1/P_2 are required. From the expressions of Appendix E, we find

$$\left(\frac{P_0}{P_1}\right)^2=\left(\frac{5\eta^2+10}{4\eta^2-2}\right)^2\left(\frac{18.0+63.6\Lambda-18.0\Lambda^2}{18.0-63.6\Lambda-18.0\Lambda^2}\right)^2,$$

$$\left(\frac{P_2}{P_1}\right)^2=\left(\frac{54-191\Lambda-72\Lambda^2+64\Lambda^3+18\Lambda^4}{98-96\Lambda-262\Lambda^2+289\Lambda^3-98\Lambda^4}\right),$$

where $\eta=c/a$, $\Lambda=\beta/\alpha$, and we have used the values of E_2 and E_5 in Fig. 3. For Λ we take the value 0.710, deduced from the work of Abragam and Boutron,[19] noting that their parameters α,β, denoted α_{AB} and β_{AB} here, are related to ours by

$$\beta/\alpha=\frac{\alpha_{AB}+\sqrt{3}\beta_{AB}}{\sqrt{3}\alpha_{AB}-\beta_{AB}}.$$

With $\eta=0.703$ we then have

$$\left(\frac{P_0}{P_1}\right)^2=8.1\times10^4; \qquad \left(\frac{P_2}{P_1}\right)^2=14.4.$$

The first is large because $4\eta^2-2$ is nearly zero with the observed value of η. These values are used in the preceding paper to evaluate the polarization ratio.

The expressions in Appendix E provide, in principle, the possibility of making a more exact estimate of the intensity than that given in the preceding section. In practice, such an estimate is made uncertain by the lack of knowledge of the wave functions (hence of X and Q) and of the real AFMR absorption intensity, which, as noted in Ref. 16, is smaller than that expected from a naive application of the Fermi golden rule. If we nevertheless employ the golden rule for the AFMR absorption and use the values $X=a_R$, $Q=a_R^2$, $a_R=0.7$ Å we find

$$\text{Intensity/AFMR}\sim10^{-2\pm2} \qquad (16)$$

from the expressions in Appendix E. Here we have used the values of α and β deduced above from the work of Abragam and Boutron and the Moriya values of the E_m's shown in Fig. 3. The result (16) is subject to great uncertainties, but seems to indicate that the proposed process may be large enough to explain the observations.

V. DISCUSSION

In this paper we have set up a model for the FeF_2 system and described a search within it for possible processes contributing to two-magnon absorption. Taking the process estimated to give the largest absorption, we derived an expression for the absorption intensity and used it to derive an equivalent "spin Hamiltonian" used in the preceding paper to derive the experimental properties of a line recently observed experimentally in the material. The expressions were used to give an estimate of the intensity ratio and somewhat more accurate estimate of the intensity, which appeared to be consistent with experiment. The search also revealed another absorption mechanism which might be giving absorption of comparable intensity to that of the process studied in detail here. A more detailed study of this process, which would probably dominate that studied here in some materials, is reserved for another communication.

We emphasize that no claim is made for the general applicability of these results to all transition-metal fluorides. In particular, we do not claim that recent experimental results of Allen *et al.*[20] on a similar line in MnF_2 can be explained on the basis of the process studied in detail in this paper. It should be noted that the line shape of the MnF_2 line is markedly different from that observed for the FeF_2 line, that the intensity is smaller by about a factor of 2, and that the polarization properties are quite different. Thus it does not appear obvious that the same process is involved in the two cases. On the other hand, in CoF_2, the spin-orbit interaction is expected to play an important role and it seems that the process considered here might be contributing to the absorption observed there by Richards.[21] No detailed experimental study of this line has appeared.

We have previously suggested[6] that a process with the same physical origin as that on which the present work is based might provide an explanation for the magnon side bands recently observed[22] in the optical-absorption spectra of MnF_2 and FeF_2. A more detailed study of this question is required before final conclusions can be drawn.

Finally, we note that the criticism of our initial proposal[6] made by Tanabe, Sugano, and Moriya[7] (TSM) does not apply to the present work, in which a different approximation is made. Previously we approximated the dipole-quadrupole interaction, written schematically $\mathbf{T}:\mathbf{Q}$, by taking the expectation value of $\mathbf{Q}$ in the ground orbital state of the system: $\mathbf{T}:\mathbf{Q}\simeq\mathbf{T}:\langle\mathbf{Q}\rangle$. TSM correctly pointed out that the linearly spin-

[19] A. Abragam and F. Boutron, Compt. Rend. **252**, 2404 (1961).

[20] S. J. Allen Jr., R. Loudon, and P. L. Richards, Phys. Rev. Letters **16**, 463 (1966).

[21] P. L. Richards, Bull. Am. Phys. Soc. **10**, 33 (1965).

[22] R. L. Greene, D. D. Sell, W. M. Yen, A. L. Schawlow, and R. M. White, Phys. Rev. Letters **15**, 656 (1965); P. G. Russell, D. S. McClure, and J. W. Stout, Phys. Rev. Letters **16**, 176 (1966).

dependent part of $\langle \mathbf{Q} \rangle$ vanishes as a consequence of the time-reversal properties of $\mathbf{L}$. This criticism does not appear to apply to the present work, in which the approximation $\mathbf{T}:\mathbf{Q} \simeq \mathbf{T}:\langle \mathbf{Q} \rangle$ is not made. TSM have proposed another microscopic explanation of the FeF_2 infrared line which is very similar to that considered independently by us in Appendix C of the present work. Our intensity estimate for this process, which was very small, cannot be regarded as conclusive. However, the contrasting experimental information on the MnF_2 and FeF_2 lines makes an explanation attributing both lines to the same mechanism seem improbable to us.

ACKNOWLEDGMENTS

The author is grateful to Professor C. Kittel, Professor M. Tinkham, and Professor C. Schwartz for advice, encouragement, and discussions, and to R. M. White, D. Mills, F. Hartman, and D. Blandin for comment and discussion. I. Silvera offered much helpful comment and discussion and Professor Friedel's group at Orsay has kindly offered hospitality while this work was completed. Dr. Richards and Professor Moriya are thanked for providing accounts of their work prior to publication.

APPENDIX A: EXCITON FORMALISM

Denote the stationary electronic orbital states of the ions by $|\Gamma_j^{mj}\rangle_a$ and $|\Gamma_{j+\tau}^{mj}\rangle_b$, where j refers to the ion site, m to the electronic energy level $E_{(m)}$, the subscripts a and b to the sublattices of the rutile structure, and τ to a translation vector carrying $a \rightarrow b$. When the crystal is in the state

$$|\{m_j\}\rangle = \sum_P (-1)^P P\{\prod_{j=1}^N |\Gamma_j^{mj}\rangle_a \prod_{j=1}^N |\Gamma_{j+\tau}^{mj}\rangle_b\},$$

where P is a permutation operator, the energy is

$$E(\{m_j\}) = \sum_{j=1}^N E(m_j) + \sum_{j=1}^N E(m_{j+\tau}).$$

We define a set of operators by

$$|\{m_j\}\rangle = \prod_{j=1}^N c(\Gamma_j^{mj})^\dagger |\mathrm{vac}\rangle; \quad c(\Gamma_j^{mj})|\mathrm{vac}\rangle = 0,$$

in terms of which the energy is

$$\sum_m E(m)[\sum_{j=1}^N c(\Gamma_j^m)^\dagger c(\Gamma_j^m) + \sum_{j=1}^N c(\Gamma_{j+\tau}^m)^\dagger c(\Gamma_{j+\tau}^m)];$$

or writing $c(\Gamma_j^m)^\dagger c(\Gamma_j^m) = n_m^{(j)}$, and introducing the low-temperature approximation $\langle n_m^{(j)} \rangle \ll 1$ for $m \neq 1$, we have, with the introduction of boson operators satisfying

$$n_m^{(j)} - n_1^{(j)} = (b_j^{(m)\dagger} b_j^{(m)} - 1),$$
$$n_m^{(j+\tau)} - n_1^{(j+\tau)} = (b_{j+\tau}^{(m)\dagger} b_{j+\tau}^{(m)} - 1),$$

that

$$\mathcal{H}_{\mathrm{ex}} = \sum_{j=1}^N \sum_{m \neq 1} E_m (b_j^{(m)\dagger} b_j^{(m)} + b_{j+\tau}^{(m)\dagger} b_{j+\tau}^{(m)}) + 2NE_1.$$

To Fourier transform the b's so that the resulting operators give eigenstates, we form

$$\beta_\lambda^{(m,a)} = \sum_{j=1}^N c_j^{(\lambda)} b_j^{(m)},$$

where λ and the C's are to be determined, and use the translational invariance of the system to find

$$C_j^{(\lambda)} = (N)^{-1/2} e^{i\mathbf{k}\cdot\mathbf{R}_j} e^{i\phi},$$

where $\mathbf{k}$ is on the reciprocal sublattice. We have then

$$\beta_{\mathbf{k}}^{(m,a)} = (N)^{-1/2} \sum_{j=1}^N e^{i\mathbf{k}\cdot\mathbf{R}_j} b_j^{(m)},$$

$$\beta_{\mathbf{k}}^{(m,b)} = (N)^{-1/2} \sum_{j=1}^N e^{i\mathbf{k}\cdot(R_j+\tau)} b_{j+\tau}^{(m)},$$

so that the Hamiltonian is

$$\mathcal{H}_{\mathrm{excitons}} = \sum_{m \neq 1} \sum_{\mathbf{k}} E_m (\beta_{\mathbf{k}}^{(m,a)\dagger} \beta_{\mathbf{k}}^{(m,a)} + \beta_{\mathbf{k}}^{(m,b)\dagger} \beta_{\mathbf{k}}^{(m,b)}).$$

APPENDIX B: PERTURBATION EXPANSION

We use standard time-dependent perturbation theory, writing the Hamiltonian in the interaction picture

$$\mathcal{H}(t) = \mathcal{H}_0(t) + \mathcal{H}_{\mathrm{I}}(t),$$

where

$$\mathcal{H}_0 = \mathcal{H}_{\mathrm{magnons}} + \mathcal{H}_{\mathrm{phonons}} + \mathcal{H}_{\mathrm{excitons}} + \mathcal{H}_{\mathrm{photons}};$$
$$\mathcal{H}_{\mathrm{I}} = \mathcal{H}_{\mathrm{mag\text{-}phon}} + \mathcal{H}_{\mathrm{ex\text{-}mag}} + \mathcal{H}_{\mathrm{ex\text{-}phon}} + \mathcal{H}_{\mathrm{ph\ t\text{-}ex}} + \mathcal{H}_{\mathrm{phon\text{-}phot}} + \mathcal{H}_{\mathrm{ex\text{-}ex}}.$$

The absorption rate is proportional to

$$\frac{d}{dt}|\langle b|\Psi(t)\rangle|^2 = \frac{d}{dt}\left|\langle b| \sum_{n=0}^\infty \left(\frac{1}{n!}\right)\left(\frac{-i}{\hbar}\right)^n \times \int_0^t \cdots \int_0^t dt_1 \cdots dt_n T\{\mathcal{H}_{\mathrm{I}}(t_1)\cdots\mathcal{H}_{\mathrm{I}}(t_n)\}|a\rangle\right|^2,$$

where T is the time-ordering operator and $|a\rangle$ contains one photon at $\mathbf{k}$, while $|b\rangle$ contains magnons at $\mathbf{k}'$ and $-\mathbf{k}'$. The series resulting from expanding the T products by use of Wick's theorem can be represented by

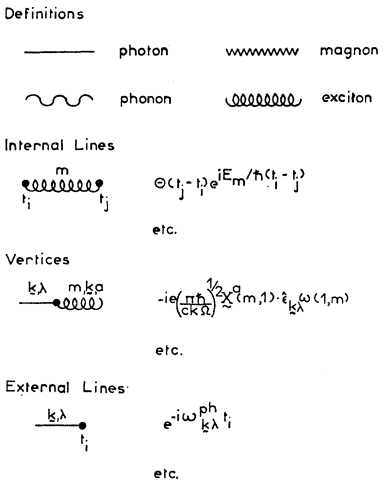

FIG. 9. Definitions of diagrams.

diagrams according to Fig. 9. Only a few representative definitions are shown.

APPENDIX C: ELECTRIC-FIELD DEPENDENCE OF THE EXCHANGE CONSTANT

We consider the states of an Fe^{2+}-F^{-}-Fe^{2+} system defined by Fig. 10. In terms of these, the J due to the usual superexchange mechanism[17] is defined as follows:

$$|1\rangle' = |1\rangle + \frac{|2\rangle\langle 2|H_{\rm tr}|1\rangle}{(E_1 - E_2)}, \tag{C1}$$

$$J = \langle 1|'H_{\rm ex}|1\rangle' = \frac{\langle 2|H_{\rm ex}|2\rangle |\langle 2|H_{\rm tr}|1\rangle|^2}{(E_1-E_2)^2}, \tag{C2}$$

where $H_{\rm tr}$ is a perturbation which connects 1 and 2, and $H_{\rm ex}$ is an operator defined so that

$$\langle 2|H_{\rm ex}|2\rangle = e^2 \int\int \varphi_d^*(\mathbf{r}_1 - \mathbf{r}_{Fe^{2+}}) \varphi_P^*(\mathbf{r}_1 - \mathbf{r}_{F^-}) r_{12}^{-1} \times \varphi_d(\mathbf{r}_2 - \mathbf{r}_{Fe^{2+}}) \varphi_P(\mathbf{r}_1 - \mathbf{r}_{F^-}) d^3r_1 d^3r_2 .$$

An effect which changes J with the application of an electric field E is found by extending the expansion (C1) to include

$$|1\rangle' = |1\rangle + \frac{|2\rangle\langle 2|H_{\rm tr}|1\rangle}{E_1-E_2} + \frac{e|2\rangle\langle 2|\mathbf{E}\cdot\mathbf{r}|3\rangle\langle 3|H_{\rm tr}'|1\rangle}{(E_1-E_2)(E_1-E_3)}, \tag{C3}$$

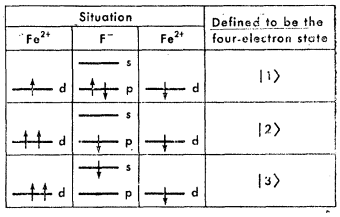

FIG. 10. Definitions of states considered in Appendix C.

where $\langle 2|\mathbf{E}\cdot\mathbf{r}|3\rangle \neq 0$ because the s and p states on the F^- ion have opposite parity. The superexchange term arising from the new term in (C3) is, to lowest order in E,

$$\left(\frac{\partial J}{\partial \mathbf{E}}\right)\cdot\mathbf{E} = \frac{\langle 3|H_{\rm tr}'|1\rangle}{\langle 2|H_{\rm tr}|1\rangle}\left(\frac{2J}{E_1-E_2}\right)\mathbf{E}\cdot\langle 2|\mathbf{r}|3\rangle .$$

The resultant intensity is of order

$$\frac{\text{Intensity from } \partial J/\partial E}{\text{AFMR}} \sim \left(\frac{2JzS}{E_1-E_2}\right)^2 10^4 \left(\frac{\langle 3|H_{\rm tr}'|1\rangle}{\langle 2|H_{\rm tr}|1\rangle}\right)^2 .$$

Taking $|E_1-E_2| \sim 10^5$ cm^{-1}; $2zJS \sim 50$ cm^{-1} we have

$$\left(\frac{\text{Intensity from } \partial J/\partial E}{\text{AFMR}}\right) \sim (2\times 10^{-3}) \left(\frac{\langle 3|H_{\rm tr}'|1\rangle}{\langle 2|H_{\rm tr}|1\rangle}\right)^2 .$$

To estimate the ratio of the matrix elements, we suppose

$$\left(\frac{\langle 3|H_{\rm tr}'|1\rangle}{\langle 2|H_{\rm tr}|1\rangle}\right)^2 \lesssim \left(\frac{S'}{S}\right)^2 ,$$

where

$$S = \int \varphi_p^*(\mathbf{r}-\mathbf{r}_{F^-}) \varphi_d(\mathbf{r}-\mathbf{r}_{Fe^{2+}}) d^3r ,$$

$$S' = \int \varphi_s^*(\mathbf{r}-\mathbf{r}_{F^-}) \varphi_d(\mathbf{r}-\mathbf{r}_{Fe^{2+}}) d^3r .$$

Choosing the p and d states to have the maximum overlap and using Slater orbitals, we estimate

$$S'/S \sim 5\times 10^{-4}.$$

Thus

$$\left(\frac{\text{Absorption for } \partial J/\partial E}{\text{AFMR}}\right) \lesssim 5\times 10^{-10}.$$

APPENDIX D: TRANSITION RATE FOR FOURTH-ORDER PROCESS

We have for the transition rate

$$W(a\to b) = \frac{2\pi}{\hbar^2}\delta(\omega_{k\lambda} - \omega_{k'+k}{}^m - \omega_{-k'}{}^m) \left| \sum_{k,l,m} \frac{\langle b|\mathcal{H}_{\rm I}|k\rangle\langle k|\mathcal{H}_{\rm I}|l\rangle\langle l|\mathcal{H}_{\rm I}|m\rangle\langle m|\mathcal{H}_{\rm I}|a\rangle}{\hbar^3 \omega_{bk}\omega_{bl}\omega_{bm}} \right|^2 . \tag{D1}$$

We can show that in all contributing processes involving the same interactions as those involved in the process of

Fig. 8(b) the intermediate states k, l, m of this sum will contain at most one exciton created by $\beta_{\mathbf{k}}^{(m,a)\dagger}$ and one exciton created by $\beta_{\mathbf{k}}^{(m,b)\dagger}$. The diagrams corresponding to the needed terms in the sum of D1 are then found by a direct calculation and we find for the sum

$$\sum_{k,l,m}\frac{\langle b|\mathcal{H}_{\mathrm{I}}|k\rangle\langle k|\mathcal{H}_{\mathrm{I}}|l\rangle\langle l|\mathcal{H}_{\mathrm{I}}|m\rangle\langle m|\mathcal{H}_{\mathrm{I}}|a\rangle}{\hbar^3\omega_{bk}\omega_{bl}\omega_{bm}}$$

$$=\sum_{m_{e'}m_0,m_{e''}}{}'\Bigg\{\frac{\lambda^2Se^3\omega(m_0,1)}{(V)^{1/2}}\left(\frac{2\pi\hbar}{\omega_{\mathbf{k}\lambda}{}^{\mathrm{ph}}}\right)^{1/2}(\sum_{\delta}{}'\sin(\mathbf{k}'\cdot\boldsymbol{\delta})\langle 1|{}_b\mathbf{Q}|m_{e'}\rangle_b:\langle m_0|{}_a\mathbf{T}_\delta|m_{e''}\rangle_a$$
$$\times\langle m_{e'}|{}_bL^-|1\rangle_b\langle m_{e''}|L^+|1\rangle_a(\mathbf{X}^{(a)}(1,m_0)\cdot\hat{\boldsymbol{\epsilon}}_{\mathbf{k}\lambda})$$
$$-\sum_{\delta}{}'\sin(\mathbf{k}'\cdot\boldsymbol{\delta})\langle 1|{}_a\mathbf{Q}|m_{e'}\rangle_a:\langle m_0|{}_b\mathbf{T}_\delta|m_{e''}\rangle_b\langle m_{e'}|{}_aL^+|1\rangle_a\langle m_{e''}|{}_bL^-|1\rangle_b(\mathbf{X}^{(b)}(1,m_0)\cdot\hat{\boldsymbol{\epsilon}}_{\mathbf{k}\lambda}))$$
$$\times([(E_{m_{e'}}+\hbar\omega_{\mathbf{k}'}{}^m)(E_{m_{e''}}+E_{m_{e'}}+\hbar\omega_{\mathbf{k}\lambda}{}^{\mathrm{ph}})(E_{m_0}+\hbar\omega_{\mathbf{k}\lambda}{}^{\mathrm{ph}})]^{-1}$$
$$-[(E_{m_0}-\hbar\omega_{\mathbf{k}\lambda}{}^{\mathrm{ph}})(E_{m_{e'}}+E_{m_{e''}}-\hbar\omega_{\mathbf{k}\lambda}{}^{\mathrm{ph}})(E_{m_{e'}}-\hbar\omega_{\mathbf{k}'}{}^m)]^{-1}$$
$$+[(E_{m_{e'}}+\hbar\omega_{\mathbf{k}'}{}^m)(E_{m_{e'}}+E_{m_0}-\hbar\omega_{\mathbf{k}\lambda}{}^{\mathrm{ph}})(E_{m_{e''}}-\hbar\omega_{\mathbf{k}'}{}^m)]^{-1}$$
$$-[(E_{m_{e''}}+\hbar\omega_{\mathbf{k}'}{}^m)(E_{m_0}+E_{m_{e'}}+\hbar\omega_{\mathbf{k}'}{}^m)(E_{m_{e'}}-\hbar\omega_{-\mathbf{k}}{}^m)]^{-1}$$
$$+[(E_{m_{e''}}+\hbar\omega_{\mathbf{k}'}{}^m)(E_{m_{e''}}+E_{m_{e'}}+\hbar\omega_{\mathbf{k}\lambda}{}^{\mathrm{ph}})(E_{m_0}+\hbar\omega_{\mathbf{k}\lambda}{}^{\mathrm{ph}})]^{-1}$$
$$-[(E_{m_0}-\hbar\omega_{\mathbf{k}\lambda}{}^{\mathrm{ph}})(E_{m_{e'}}+E_{m_{e''}}-\hbar\omega_{\mathbf{k}\lambda}{}^{\mathrm{ph}})(E_{m_{e''}}-\hbar\omega_{\mathbf{k}'}{}^m)]^{-1})$$
$$+\frac{\lambda^2Se^3\omega(m_{e''},m_0)}{(V)^{1/2}}\left(\frac{2\pi\hbar}{\omega_{\mathbf{k}\lambda}{}^{\mathrm{ph}}}\right)^{1/2}(\sum_{\delta}{}'\sin(\mathbf{k}'\cdot\boldsymbol{\delta})\langle 1|{}_b\mathbf{Q}|m_{e'}\rangle_b:\langle 1|{}_aT_\delta|m_0\rangle_a$$
$$\times\langle m_{e''}|{}_aL^+|1\rangle_a\langle m_{e'}|{}_bL^-|1\rangle_b(\mathbf{X}^{(a)}(m_0,m_{e'})\cdot\hat{\boldsymbol{\epsilon}}_{\mathbf{k}\lambda})$$
$$-\sum_{\delta}{}'\sin(\mathbf{k}'\cdot\boldsymbol{\delta})\langle 1|{}_a\mathbf{Q}|m_{e'}\rangle_a:\langle 1|{}_b\mathbf{T}_\delta|m_0\rangle_b\langle m_{e'}|{}_aL^+|1\rangle_a\langle m_{e''}|{}_bL^-|1\rangle_b(\mathbf{X}^{(b)}(m_0,m_{e''})\cdot\hat{\boldsymbol{\epsilon}}_{\mathbf{k}\lambda})$$
$$\times([(E_{m_{e'}}+\hbar\omega_{\mathbf{k}'}{}^m)(E_{m_{e'}}+E_{m_{e''}}+\hbar\omega_{\mathbf{k}\lambda}{}^{\mathrm{ph}})(E_{m_0}+E_{m_{e'}})]^{-1}$$
$$-[(E_{m_0}+E_{m_{e'}})(E_{m_{e''}}+E_{m_{e'}}-\hbar\omega_{\mathbf{k}\lambda}{}^{\mathrm{ph}})(E_{m_{e'}}-\hbar\omega_{\mathbf{k}'}{}^m)]^{-1}$$
$$+[(E_{m_{e'}}+\hbar\omega_{\mathbf{k}'}{}^m)(E_{m_0}+\hbar\omega_{\mathbf{k}'}{}^m)(E_{m_{e''}}-\hbar\omega_{\mathbf{k}'}{}^m)]^{-1}$$
$$-[(E_{m_{e''}}+\hbar\omega_{\mathbf{k}'}{}^m)(E_{m_0}-\hbar\omega_{\mathbf{k}'}{}^m)(E_{m_{e'}}-\hbar\omega_{\mathbf{k}'}{}^m)]^{-1}$$
$$+[(E_{m_{e''}}+\hbar\omega_{\mathbf{k}'}{}^m)(E_{m_{e''}}+E_{m_{e'}}+\hbar\omega_{\mathbf{k}\lambda}{}^{\mathrm{ph}})(E_{m_0}+E_{m_{e'}})]^{-1}$$
$$-[(E_{m_0}+E_{m_{e'}})(E_{m_{e''}}+E_{m_{e'}}-\hbar\omega_{\mathbf{k}\lambda}{}^{\mathrm{ph}})(E_{m_{e''}}-\hbar\omega_{\mathbf{k}'}{}^m)]^{-1})\Bigg\}. \quad \text{(D2)}$$

Here we have used $\omega_{\mathbf{k}\lambda}{}^{\mathrm{ph}}=\omega_{\mathbf{k}'+\mathbf{k}}{}^m+\omega_{-\mathbf{k}'}{}^m$, as required by the delta function, and have assumed $|\mathbf{k}'|\gg|\mathbf{k}|$, $\omega_{\mathbf{k}'}{}^m=\omega_{-\mathbf{k}'}{}^m$. With the approximations allowed by $\hbar\omega_{\mathbf{k}\lambda}{}^{\mathrm{ph}}\ll E_{m_{e'}},E_{m_{e''}}$; $E_{m_{e'}}\ll E_{m_0}$, one finds (13).

APPENDIX E: CALCULATION OF MATRIX ELEMENTS FOR FeF_2

We define

$$M^{(1)}(m_{e'},m_{e''},m_0)=\left[\frac{1}{E_{m_0}}\left(\frac{5E_{m_{e'}}E_{m_{e''}}+3E_{m_{e'}}{}^2+2E_{m_{e''}}{}^2}{E_{m_{e'}}{}^2(E_{m_{e'}}+E_{m_{e''}})^2E_{m_{e''}}}\right)+\frac{1}{E_{m_0}{}^2}\left(\frac{5E_{m_{e'}}E_{m_{e''}}{}^2+E_{m_{e'}}{}^3+2E_{m_{e'}}{}^2E_{m_{e''}}+E_{m_{e''}}{}^3}{E_{m_{e'}}(E_{m_{e'}}+E_{m_{e''}})^2(E_{m_{e''}})^2}\right)\right],$$

$$M^{(2)}(m_{e'},m_{e''},m_0)=\left[\frac{1}{E_{m_0}}\left(\frac{5E_{m_{e'}}E_{m_{e''}}+3E_{m_{e''}}{}^2+2E_{m_{e'}}{}^2}{E_{m_{e''}}{}^2(E_{m_{e'}}+E_{m_{e''}})^2E_{m_{e'}}}\right)+\frac{1}{E_{m_0}{}'{}^2}\left(\frac{-6E_{m_{e'}}E_{m_{e''}}{}^2+3E_{m_{e'}}{}^2E_{m_{e''}}+E_{m_{e'}}{}^3-2E_{m_{e''}}{}^3}{E_{m_{e'}}(E_{m_{e'}}+E_{m_{e''}})^2E_{m_{e''}}{}^2}\right)\right],$$

$$Q=\int_0^\infty r^4f_d{}^2(r)dr, \quad \text{and} \quad X=\int_0^\infty r^3f_d(r)f_p(r)dr.$$

In the last expressions we consider only the electron outside the closed half-shell of the Fe^{2+} ion and write the wave functions indicated in Fig. 3 as

$$|xy\rangle=(15/4\pi)^{1/2}(xy/r)f_d(r); \qquad |xz\rangle=(15/4\pi)^{1/2}(xz/r)f_d(r);$$
$$|3z^2-r^2\rangle=(5/16\pi)^{1/2}[(3z^2-r^2)/r^2]f_d(r); \quad |x^2-y^2\rangle=(15/16\pi)^{1/2}[(x^2-y^2)/r^2]f_d(r);$$
$$|p_z\rangle=(3/4\pi)^{1/2}(z/r)f_p(r); \quad |p_x\rangle=(3/4\pi)^{1/2}(x/r)f_p(r); \quad |p_y\rangle=(3/4\pi)^{1/2}(y/r)f_p(r).$$

Then, doing the angular integrals and calculating the matrix elements of L, one finds from Eq. (13) the following expressions for the three possible polarizations of the electric field:

$$\sum_{k,l,m}\frac{\langle b|\mathcal{H}_I|k\rangle\langle k|\mathcal{H}_I|l\rangle\langle l|\mathcal{H}_I|m\rangle\langle m|\mathcal{H}_I|a\rangle}{\hbar^3\omega_{bk}\omega_{bl}\omega_{bm}}$$
$$=\frac{\lambda^2Se^3\hbar\omega_{k\lambda}{}^{ph}}{210(V)^{1/2}}\left(\frac{6\pi\hbar}{\omega_{k\lambda}{}^{ph}}\right)^{1/2}X^2Q\sum_\delta{}'\sin(\mathbf{k}'\cdot\boldsymbol{\delta})\times\frac{\delta_z}{|\boldsymbol{\delta}|^5}\left[\left(\frac{5\delta_y{}^2}{|\boldsymbol{\delta}|^2}-1\right)\mathfrak{M}(z;y)+\left(\frac{5\delta_x{}^2}{|\boldsymbol{\delta}|^2}-1\right)\mathfrak{M}(z;x)\right]; \quad \mathbf{E}\|z \text{ axis}$$
$$\times\left(\frac{5\delta_z{}^2}{|\boldsymbol{\delta}|^2}-1\right)\left[\frac{\delta_y}{|\boldsymbol{\delta}|^5}\mathfrak{M}(x;y)+\frac{\delta_x}{|\boldsymbol{\delta}|^5}\mathfrak{M}(x;x)\right]; \quad \mathbf{E}\|x \text{ axis};$$
$$\times\left(\frac{5\delta_z{}^2}{|\boldsymbol{\delta}|^2}-1\right)\left[\frac{\delta_y}{|\boldsymbol{\delta}|^5}\mathfrak{M}(y;y)+\frac{\delta_x}{|\boldsymbol{\delta}|^5}\mathfrak{M}(y;x)\right]; \quad \mathbf{E}\|y \text{ axis}.$$

Here (the arguments of $M^{(i)}(m_e;m_{e''},m_0)$ and $\omega(m_{e'},m_0)$ refer to Fig. 3)

$$\begin{aligned}
\mathfrak{M}(z;y)&=-(3\alpha^2-\beta^2)\{(\alpha^2-3\beta^2)(M^{(2)}(2,5,8)\omega(5,8)-M^{(2)}(5,2,7)\omega(2,7))\\
&\quad+2\alpha((\alpha+\sqrt{3}\beta)M^{(1)}(2,5,6)\omega(6,1)-(\alpha-\sqrt{3}\beta)M^{(1)}(5,2,6)\omega(6,1)\};\\
\mathfrak{M}(x;y)&=i(\alpha+\sqrt{3}\beta)^2(\sqrt{3}\alpha-\beta)^2M^{(1)}(2,2,7)\omega(7,1)+i(\alpha-\sqrt{3}\beta)^2(\sqrt{3}\alpha+\beta)^2M^{(1)}(5,5,8)\omega(8,1)\\
&\quad+2i\alpha[(\alpha+\sqrt{3}\beta)(\sqrt{3}\alpha-\beta)^2M^{(2)}(2,2,6)\omega(2,6)+(\alpha-\sqrt{3}\beta)(\sqrt{3}\alpha+\beta)M^{(2)}(5,5,6)\omega(5,6)];\\
\mathfrak{M}(x;x)&=(3\alpha^2-\beta^2)(\alpha^2-3\beta^2)[M^{(1)}(2,5,8)\omega(8,1)-M^{(1)}(5,2,7)\omega(7,1)]\\
&\quad+2\alpha(3\alpha^2-\beta^2)[(\alpha+\sqrt{3}\beta)M^{(2)}(2,5,6)\omega(5,6)-(\alpha-\sqrt{3}\beta)M^{(2)}(5,2,6)\omega(2,6)].
\end{aligned} \tag{E1}$$

The relations

$$\mathfrak{M}(z;y)=-\mathfrak{M}(z;x); \quad \mathfrak{M}(x;y)=-\mathfrak{M}(y;x); \quad \mathfrak{M}(x;x)=-\mathfrak{M}(y;y)$$

follow from direct calculation. The transition rate can thus be written in the form shown in Eq. (15), where

$$\begin{aligned}
P_0&=\frac{-\lambda^2Se^3\sqrt{3}}{210(4S)}X^2Q\frac{5}{|\boldsymbol{\delta}|^7}\mathfrak{M}(z;x);\\
iP_2&=\frac{-\lambda^2Se^3\sqrt{3}}{210(4S)}X^2Q\frac{1}{|\boldsymbol{\delta}|^7}\left(\frac{5\delta_z{}^2}{|\boldsymbol{\delta}|^2}-1\right)\mathfrak{M}(x;y);\\
P_1&=\frac{-\lambda^2Se^3\sqrt{3}}{210(4S)}X^2Q\frac{1}{|\boldsymbol{\delta}|^7}\left(\frac{5\delta_z{}^2}{|\boldsymbol{\delta}|^2}-1\right)\mathfrak{M}(x;x).
\end{aligned} \tag{E2}$$